Supporting Information

Hierarchy of Interfacial Passivation in Inverted Perovskite Solar Cells

Tun Wang, Sadeq Abbasi, Xin Wang, Yangrunqian Wang, Zhendong Cheng, Jiayuan Wang, Hong Liu, Wenzhong Shen**

Key Laboratory of Artificial Structures and Quantum Control (Ministry of Education), Institute of Solar Energy, School of Physics and Astronomy, Shanghai Jiao Tong University, Shanghai 200240, P. R. China

1. Experimental Section

1.1. Solution preparation. The perovskite precursor solution was prepared by dissolving 461 mg of PbI_2 and 159 mg of CH_3NH_3I (molar ratio 1:1) in 1 mL of mixed γ-butyrolactone (GBL) and dimethyl sulfoxide (DMSO) solvent (7:3 v/v). Polystyrene (or polymethyl methacrylate) and polymethyl methacrylate (PMMA) were separately dissolved in chlorobenzene (CB) by magnetic stirring for 2 hours with different concentrations (0.2, 0.5, 1.0, 2.0 and 5.0 mg mL^{-1}). Phenyl-C61-butyric acid methyl ester (PCBM) was also dissolved in chlorobenzene with a concentration of 20 mg mL^{-1}. Nickel nitrate was dissolved in the deionized water with a molar concentration of 0.02 M.

1.2. Perovskite solar cell fabrication. Firstly, the etched FTO/glass substrates were sequentially cleaned by sonication in acetone, isopropanol, ethanol and deionized water

for 15 min, respectively. Then, the NiO_x film was fabricated by electrochemical deposition method using an electrochemical workstation (CS350H, Corrtest, China) and the details have been reported by our previous works.[1,2] Thereafter, the lower passivation layer was prepared by spin-coating the passivator precursor (PS or PMMA solution) on the NiO_x film at 4000 rpm for 30 s and then annealing at 70 °C for 10 min on a hot plate. Subsequently, the perovskite precursor solution was spin-coated onto the passivation layer at 500 rpm for 12 s and then at 4000 rpm for 30 s. Afterwards, 150 μL chlorobenzene was quickly dropped onto the center of the substrate at 10 s before the end of the spin-coating process. Then the samples were placed in an airtight glass tank and annealed for 10 min at 100 °C to remove the solvent residues. The perovskite layer with upper passivation layer was prepared by directly spin-coating the perovskite precursor solution on the NiO_x film at 500 rpm for 12 s and then at 4000 rpm for 30 s. This time 150 μL passivator precursor was quickly dropped onto the substrate at 10 s before the end of the process. As for the pristine device, the perovskite film was also prepared on the NiO_x ETL without any passivation layers, where the chlorobenzene worked as the antisolvent. Then the PCBM solution was deposited on perovskite layer by spin-coating at 2000 rpm for 30 s. All the solutions have been filtered through polytetrafluoroethylene (TPFE) filters (0.45 μm) before each spin-coating process. Finally, silver electrodes were deposited by thermal evaporation (PECVD350, Shenyang Xinlantian vacuum technology Co., Ltd, China). The active area of the fabricated PSC devices is 0.25 cm^2. The hole-only devices were fabricated with structures of FTO/NiO_x/$CH_3NH_3PbI_3$/Ag (pristine), FTO/NiO_x/PS/$CH_3NH_3PbI_3$/Ag

(lower passivated) and FTO/NiO_x/$CH_3NH_3PbI_3$/PS/Ag (upper passivated), respectively.

1.3. Characterizations. The morphologies of the NiO_x and perovskite films were characterized by scanning electron microscopy (SEM, Carl Zeiss, Germany) and atomic force microscopy (AFM, Nanoscope IIIa Multimode, USA). The transmission spectra of the NiO_x films and absorption spectra of the perovskite layers were collected by UV/vis/NIR spectrophotometer (LAMBDA750, PerkinElmer, USA). The crystallinity of the perovskite film was characterized by X-ray diffraction (XRD, D8 ADVANCE, Germany). A contact angle analyzer (DSA100, KRÜSS, Germany) was used to measure the surface wettability of the prepared passivation layer. Furthermore, the steady-state photoluminescence (PL) and time-resolved photoluminescence (TRPL) spectra of the samples were measured by Steady-State & Time-Resolved Fluorescence Spectrofluorometer (QM/TM/IM, PTI, USA) with an excitation laser of 460 nm. The photocurrent density-voltage (*J-V*) characteristics of the as-fabricated devices were tested under standard 1 sun AM 1.5G by a solar simulator (Newport, 2612A) in air, with scanning rate of 100 mV/s. The solar simulator has been calibrated with a Newport 91150 V reference silicon cell system before measurement. The external quantum efficiency (EQE) spectra of PSCs were measured using a quantum efficiency measurement system (QEX10, PV measurements, USA) in air. An electrochemical workstation (CS350H, Corrtest, China) was used to measure the electrochemical impedance spectroscopy (EIS) and Mott-Schottky characterizations.

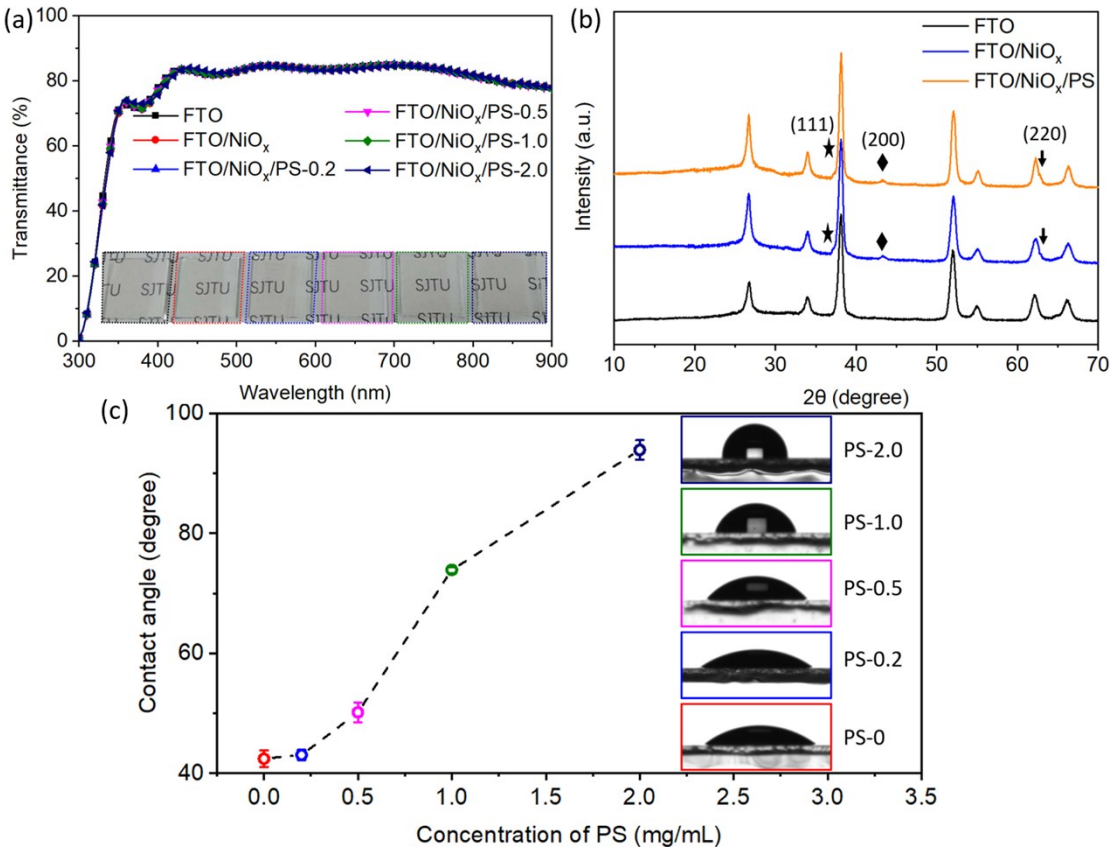

Fig. S1 (a)The schematic procedure for preparing perovskite films with lower and upper passivation layer. (b) XRD patterns of pristine FTO substrate, NiO_x film before and after depositing with PS layer. (c) Surface contact angles of FTO/NiO_x samples deposited with different PS concentration. The numbers indicate the PS concentration in mg mL^{-1}.

The FTO/NiO_x/PS sample shows very similar X-ray diffraction (XRD) pattern and transmittance spectra with that of the FTO/NiO_x sample and does not show any significant additional peaks related to PS (around 20°),[3] which could be due to the ultrathin thickness of the PS passivation layer (Fig. S1a-b). As exhibited in our previous publication,[1] the FTO grains were totally covered by mesoporous NiO_x film, which was prepared by electrochemical deposition method. Besides, because of poor electrical

conductivity of PS material, the NiO_x film was gradually covered by a hazy PS layer with the increasing PS concentration from 0 to 0.2, 0.5, 1.0, and 2.0 mg mL^{-1}, respectively. Furthermore, the contact angle against water of the PS layer surface can become larger with the increasing PS concentration (Fig S1c),[4] which will be beneficial for perovskite growth because of lower surface tension, thus promoting the charge extraction and transport between perovskite and NiO_x layer.[5]

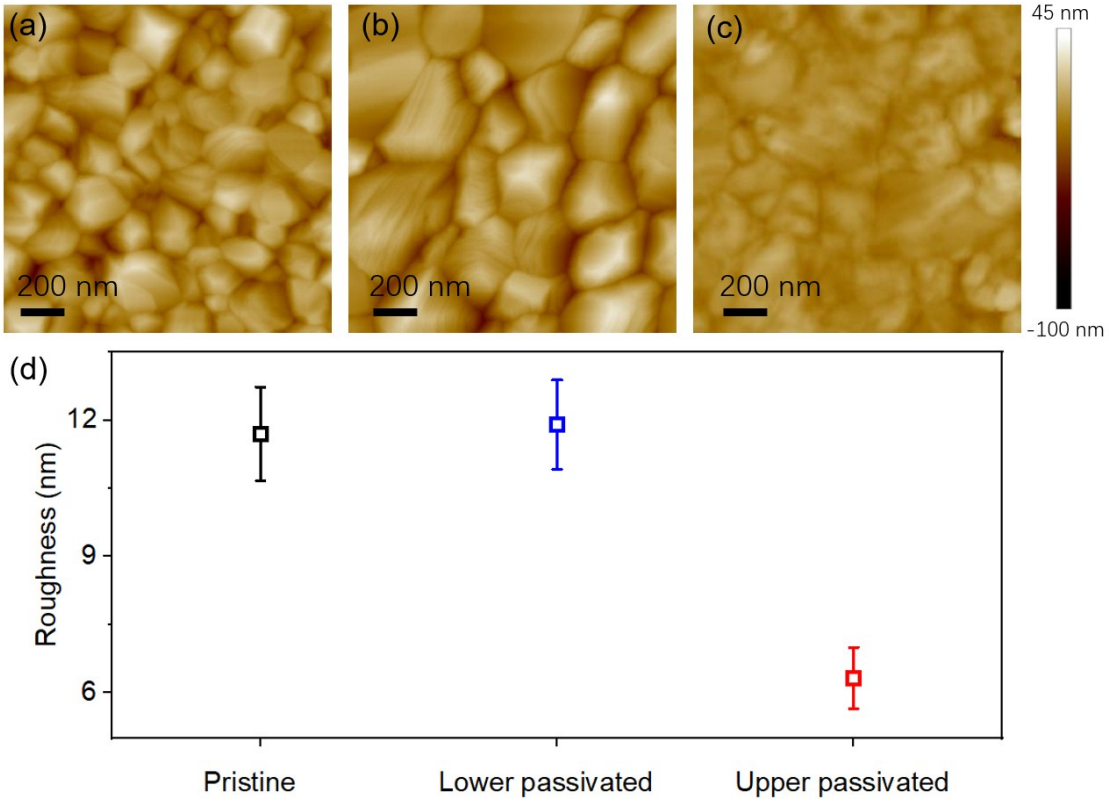

Fig. S2 AFM images of the upper surface of (a) the pristine, (b) lower passivated and (c) upper passivated perovskite films (passivated by PS). (d) Statistics of surface roughness of the corresponding perovskite films.

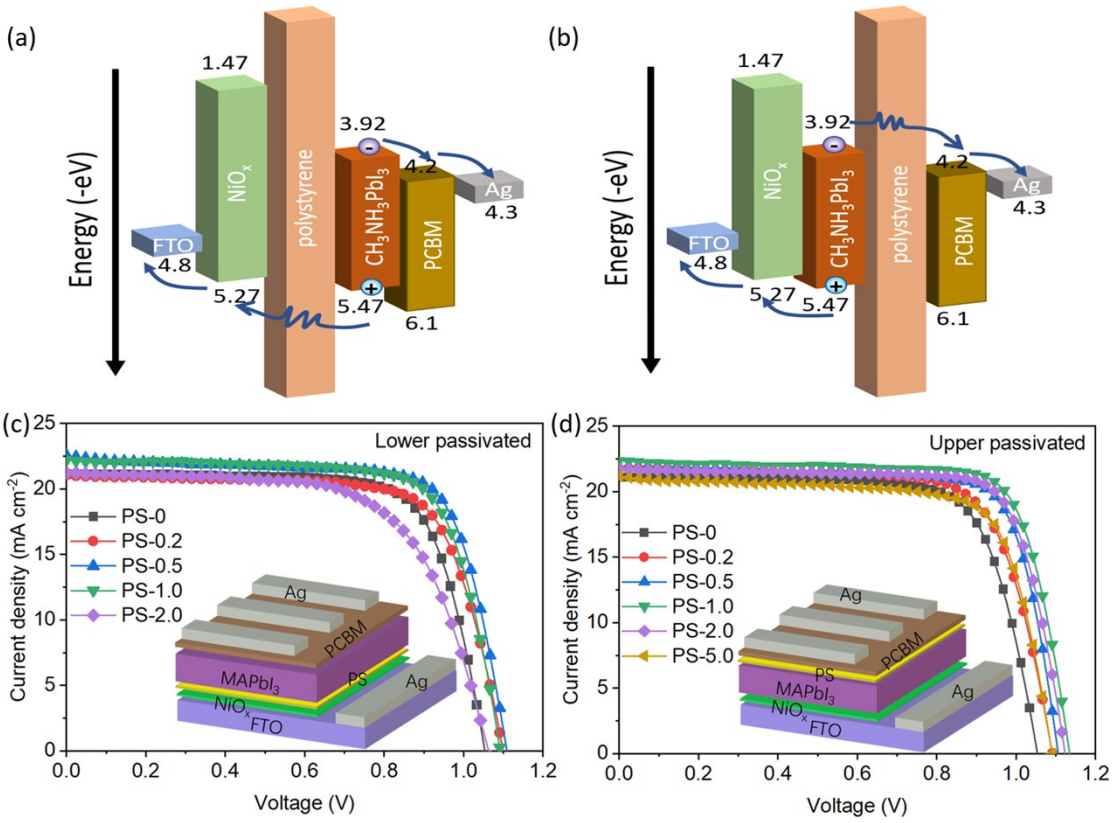

Fig. S3 Energy level diagrams of (a) lower passivated and (b) upper passivated solar cells. *J-V* curves of PSCs based on (c) lower and (d) upper passivation layer with different PS concentrations.

Table S1. Photovoltaic parameters of the PSCs based on lower passivation layer at various concentrations of PS solution.

C_{PS} (mg mL^{-1})	V_{OC} (V)	J_{SC} (mA cm^{-2})	FF (%)	PCE (%)
0	1.052	21.12	73.76	16.39
0.2	1.099	21.12	72.85	16.91
0.5	1.108	22.45	73.94	18.39
1.0	1.092	22.10	74.36	17.95
2.0	1.062	21.22	64.31	14.49

Table S2. Photovoltaic parameters of the PSCs based on upper passivation layer at various concentrations of PS solution.

C_{PS} (mg mL^{-1})	V_{OC} (V)	J_{SC} (mA cm^{-2})	FF (%)	PCE (%)
0	1.052	21.12	73.76	16.39
0.2	1.091	21.84	75.52	17.27
0.5	1.105	21.89	76.57	18.51
1.0	1.133	22.29	77.43	19.55
2.0	1.121	21.71	77.61	18.89
5.0	1.090	21.04	74.04	16.98

Table S3. Photovoltaic parameters of the PSCs with or without PS passivation layers

Sample	Scan direction	V_{OC} (V)	J_{SC} (mA cm^{-2})	FF (%)	PCE (%)
Pristine	Reverse	1.052	21.12	73.76	16.39
	Forward	1.050	21.10	72.77	16.12
Lower passivated	Reverse	1.108	22.45	73.94	18.39
	Forward	1.109	22.43	73.25	18.22
Upper passivated	Reverse	1.133	22.29	77.43	19.55
	Forward	1.131	22.19	77.76	19.52

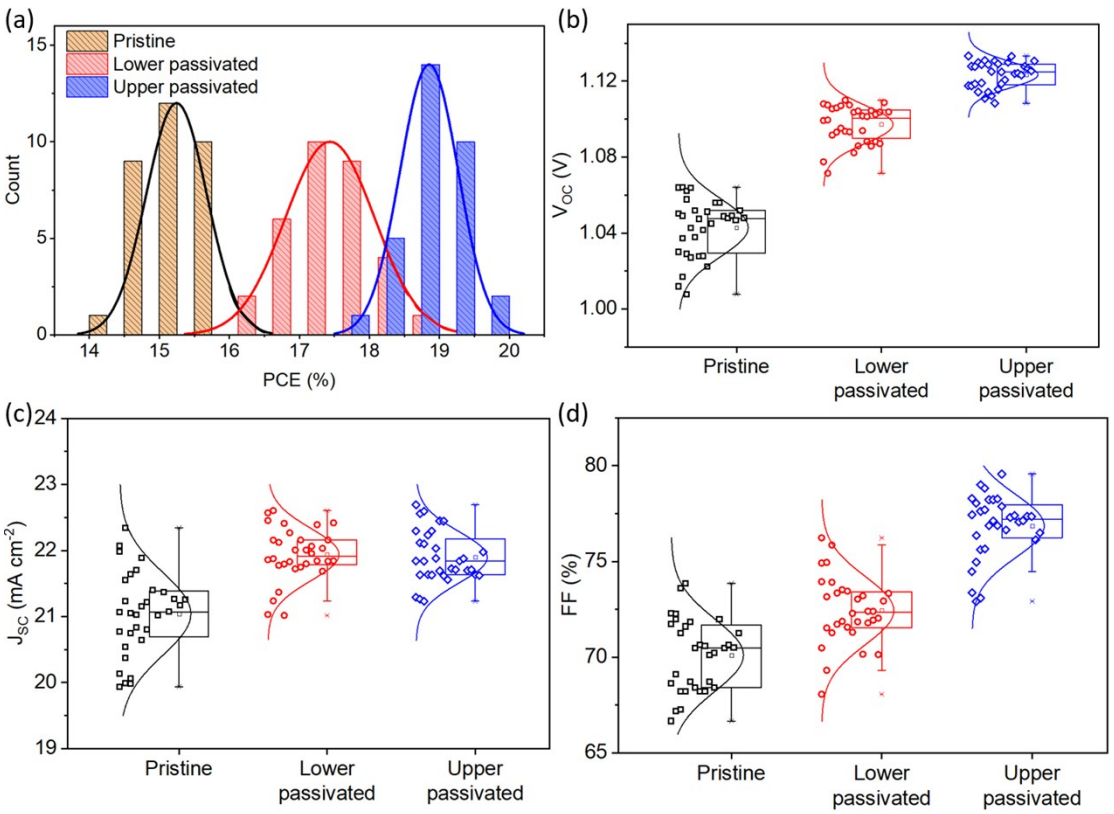

Fig. S4 Statistics of (a) PCE, (b) V_{OC}, (c) J_{SC} and (d) FF measured for samples with different passivation conditions (sample number 32 for each condition).

The histograms of PCE clearly indicate best performance in PSCs with upper passivation layer and the average value is 18.85% ± 0.41%, which is much better than the values of 15.25% ± 0.45% and 17.44% ± 0.62% for the pristine and lower passivated devices, demonstrating high reproducibility and photovoltaic performance (Fig. S4). The results also indicate the significant increase of PCE for the upper passivated devices is mainly attributed to the improvement V_{OC} and FF, which should be attributed to better quality of perovskite film and suppressed recombination of photoinduced carriers at the interfaces between perovskite and hole/electron transport layers due to appropriate passivation.[6]

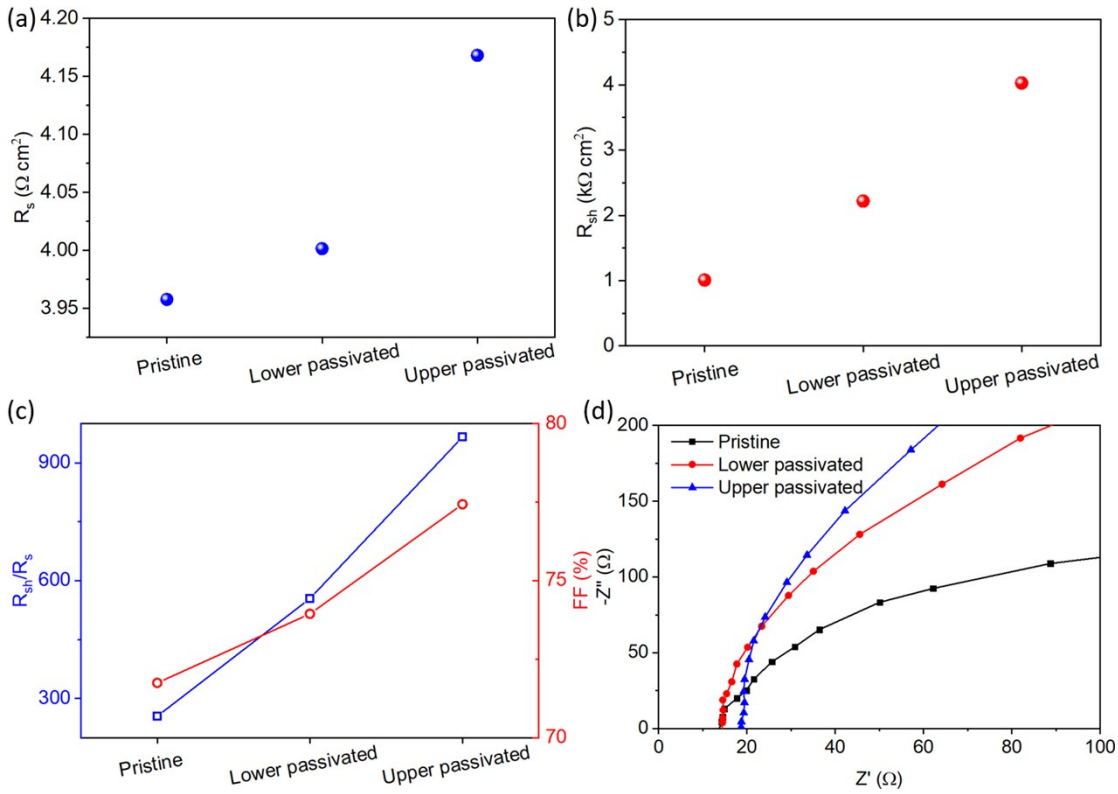

Fig. S5 (a) R_s and (b) R_{sh} and (c) R_{sh}/R_s and FF for the reference, lower passivated and upper passivated devices. (b) Enlarged view of the left part of EIS plot shown in Figure 6a.

Table S4. Summary of the fitted parameters of the TRPL decay traces.

Sample	A_1 (%)	τ_1 (ns)	A_2 (%)	τ_2 (ns)	τ_a (ns)
Pristine	66.6	5.1	33.4	17.9	13.3
Lower passivated	89.6	3.6	10.4	11.7	5.8
Upper passivated	60.8	3.6	39.2	18.5	15.1

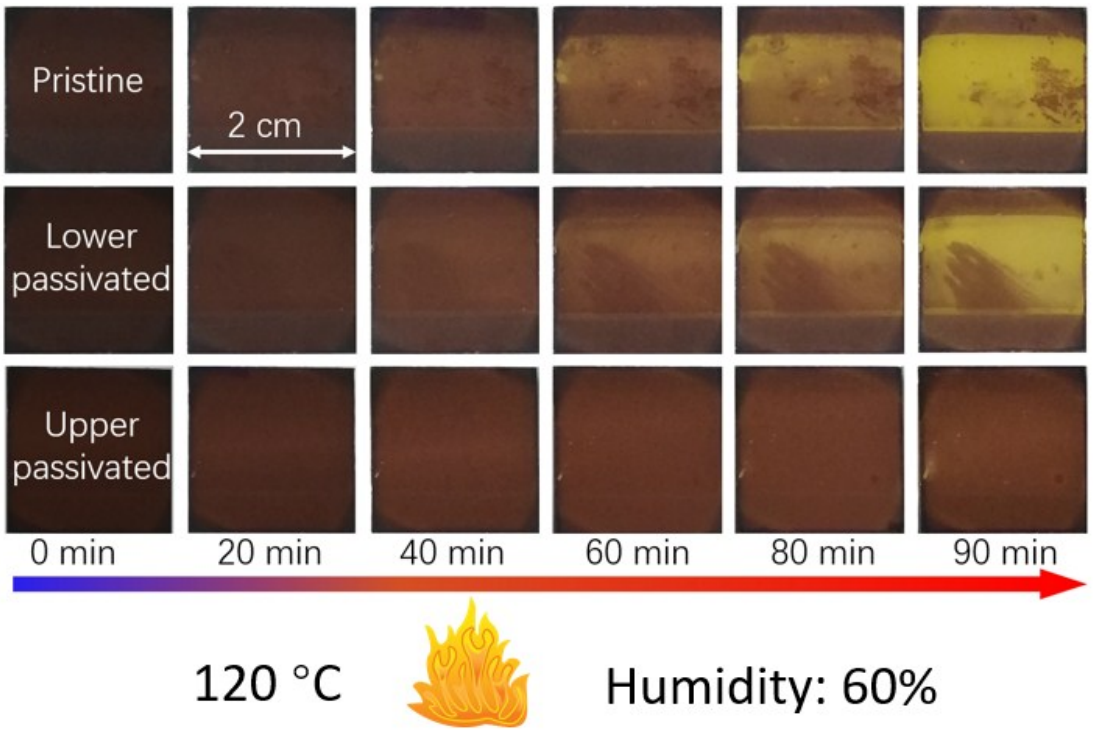

Fig. S6 Photographs of perovskite films without and with lower and upper passivation layer annealed for different times at 120 °C in air.[4]

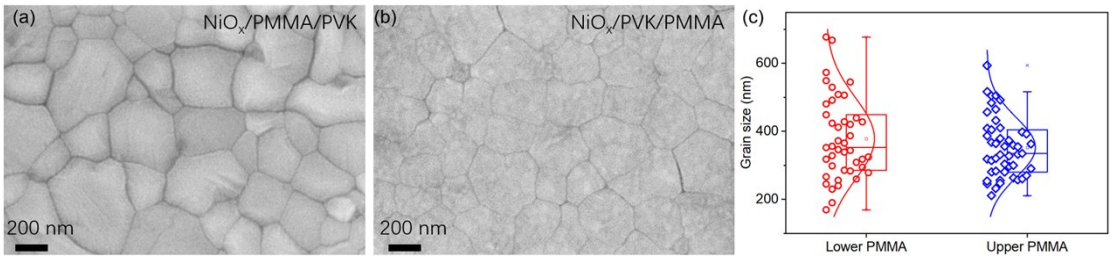

Fig. S7 SEM images of perovskite films passivated by (a) lower PMMA layer and (b) upper PMMA layer. (c) Statistic diagram of perovskite grain size.

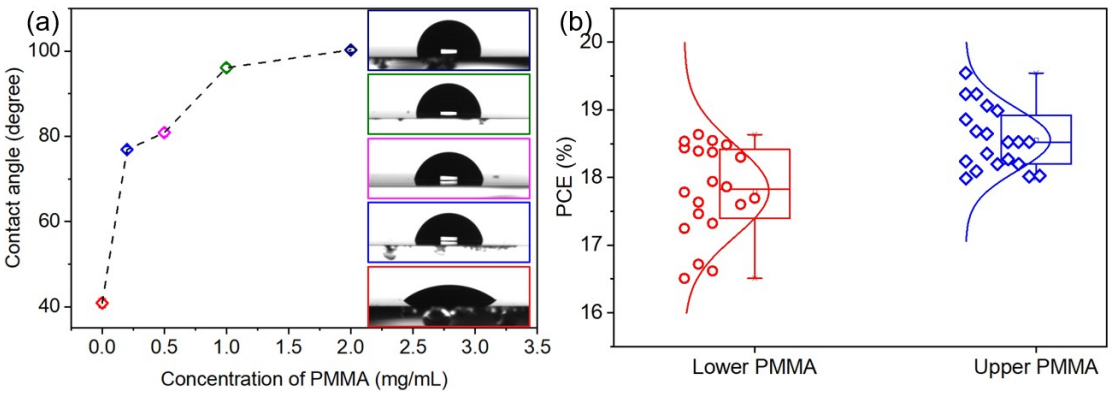

Fig. S8 (a) Contact angles of a water droplet on NiO_x/PMMA surfaces with different concentrations of PMMA solution. The insets are the real optical images of the water droplets. (d) Statistics of PCEs measured for samples with different passivation conditions.

References

1 T. Wang, D. Ding, X. Wang, R. Zeng, H. Liu and W. Shen, *ACS Omega*, 2018, **3**, 18434-18443.

2 T. Wang, D. Ding, H. Zheng, X. Wang, J. Wang, H. Liu and W. Shen, *Sol. RRL*, 2019, **3**, 1900045.

3 H. Xuemei and Y. Hao, *J. Nanomater.*, 2013, **2013**, 1-8.

4 T. Wang, Z. Cheng, Y. Zhou, H. Liu and W. Shen, *J. Mater. Chem. A*, 2019, **7**, 21730-21739.

5 Y. Wang, W. Fu, J. Yan, J. Chen, W. Yang and H. Chen, *J. Mater. Chem. A*, 2018, **6**, 13090-13095.

6 Y. Zhang, S. Zhang, S. Wu, C. Chen, H. Zhu, Z. Xiong, W. Chen, R. Chen, S. Fang and W. Chen, *Adv. Mater. Interfaces*, 2018, **5**, 1800645.